THIN JOINT CONCRETE BLOCKWORK IN FLEXURE: TESTING PROGRAMME AND RESULTS

O.J. Kanyeto, MBIE, MIMS and A.N. Fried, CEng., MICE, FIMS
[1]Lecturer, Department of Civil Engineering, University of Botswana, Gaborone, Botswana, kanyetoo@mopipi.ub.bw
[2] Senior Lecturer, Department of Civil and Space Structures, University of Surrey, UK, A.Fried@surrey.ac.uk

ABSTRACT
The transverse lateral load capacity of masonry built using solid dense concrete blocks with thin joint mortar is up to 3.5 times that of similar blockwork constructed using conventional mortar. Both the mortar properties and the constituents of the parent material forming the block alter the joint strength resulting in enhancements to tensile flexural bond strength. Essentially when thin joint technology is employed, in conjunction with solid dense concrete blocks, the masonry behaves more as a concrete plate than conventional blockwork. A testing programme was undertaken at Kingston University to ascertain this trend, and its results are presented in this paper. Two concrete block types and one thin layer mortar type were used to build wall panels which were then tested to failure. Graphs plotted from the test data reveal a linear relationship between the load and displacement, from initial application of the load until failure. This paper reports on the testing programme that was undertaken by Kingston University Sustainable Technology Research Group.

KEYWORDS: thin joint, bond strength, load capacity, elastic behaviour, conventional masonry

1.0 INTRODUCTION
Unreinforced masonry design in the UK is currently undertaken in accordance with BS5628: Part 1:1992, the code of practice for structural use of unreinforced masonry [1]. This code is for structures designed using conventional masonry, and excludes thin joint mortars. Thin joint mortar technology utilises a cementitious mortar but with polymers included to bond units together. In accordance with EC6 [2], thin joints should be under 3.0mm in thickness but this is insufficient to allow for variations in block size and 5.0mm is a practical minimum with normal unit tolerances. Modern developments in masonry construction include structures constructed using thin joint mortar, which offers three main advantages to designers.

Firstly, when thin joint mortar is used in conjunction with Aircrete it reduces the joint volume considerably. Heat flow through masonry formed using Aircrete blocks is predominantly through the mortar joints so reducing their thickness will improve a wall's thermal resistance. Thin joint masonry is currently widely used in industry in association with Aircrete blocks for this reason but the technology, particularly in the UK, is rarely associated with solid dense concrete blocks or brickwork.

Secondly, the nature of the mortar and constituents of the material forming the block significantly enhance bond strength to the point where, in many instances, it exceeds block unit modulus of rupture (UMOR) [3]. For that reason, wall panels formed using thin joint masonry have lateral capacities dependant on the UMOR, not the tensile bond strength of the joint. Consequently, load capacity of walls built using thin joint technology in conjunction with solid dense concrete blocks or bricks with high UMOR's will be considerably higher than if the walls had been built using conventional mortar.

Lastly, in addition to enhanced mechanical properties, thin joint masonry can provide designers with an improved degree of confidence in their design as compared to conventional masonry. Physical tests on wall panels constructed using thin joint technology have produced values of strength properties that have less variability than those obtained from conventional masonry tests. The variability of strength properties between identical panels is not as considerable as in conventional masonry. Hence, it may be feasible to reduce partial safety factors for materials when using thin joint mortar.

2.0 THE TESTS

Laboratory testing included 24 wallette specimens and two walls constructed using solid concrete blocks built using thin joint mortar. All blocks were 440mm long x 100mm wide x 215mm deep. Half of the specimens (one wall and twelve wallettes) were constructed using a "grey" block of strength 20N/mm^2 and density 1700kg/m^3 whilst the remainder were built using a "yellow" block of strength 14N/mm^2 and density 1400kg/m^3. Walls measured 2.65 x 1.75m and the wallettes were either 1.5 units long x 5 units high (665 x 1095mm) when tested about an axis parallel to the bed joints or 2.5 units long x 4 units high (1100 x 875mm high) when tested about an axis perpendicular to the bed joints. Specimens were all built by an experienced mason at a brick/block producer in the Midlands in order to assess the potential of the process for prefabrication demonstrated by then transporting the specimens by lorry to Kingston University in SW London. The specimens were stored in the laboratory prior to testing. The age of the mortar and specimens exceeded 28 days in all cases.

2.1 WALLETTE TESTING

The sizes of the wallettes, as well as the testing procedure, complied with the recommendations of the British Standards Institution as outlined in BS 5628 Part 1, Appendix A.3 [1], and conformed to BS ENV: Part 2 [2] .

In addition to the standard flexural test arrangement, deflection data was also obtained. Linear Variable Differential Transducers (LVDT's) were located at three points on each wallette, one near the mid-span and one near each support, see Figure 2.1. Magnetic bases attached the LVDT's to unloaded elements of the test rig. Loading was applied at a slow and repeatable rate using an hydraulic jack until failure of the specimen. With each test, the panel was initially loaded to 1 kN and left for 60 seconds before additional loading was applied. Displacement data was continuously gathered by data logger but only corroborated to load values at intervals of 0.5 kN. With displacements recorded at three different points it was possible to calculate curvatures of the wallettes at different levels of stress.

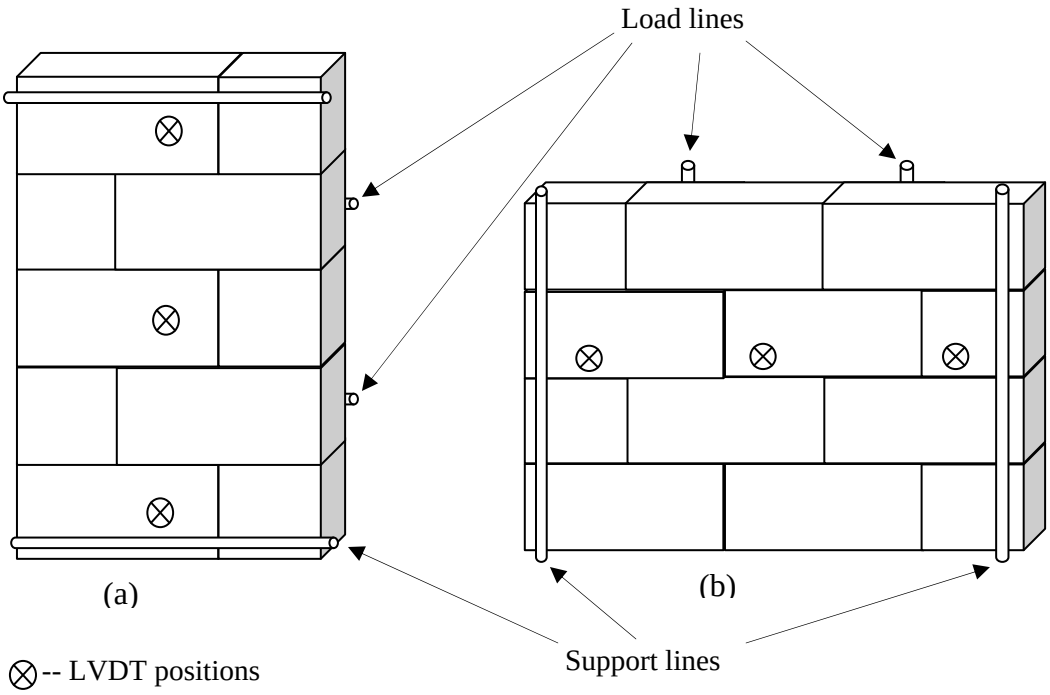

Figure 2.1: Block wallettes showing positions of LVDT's; (a) for vertical bending test, (b) for horizontal bending test

2.2 WALL TESTING

Figure 2.2 and section AA indicate a schematic view and section of the wall testing rig, with a wall in place. The all round simple support for the wall was provided using rubber hose attached to the bearing face of the test frame along all edges. The base of the wall was supported on a metal bearer designed to enable the wall to move laterally without restraint. Loading to the wall was uniformly distributed and provided by an air bag of similar area to the wall. Pressure was supplied by a pump and a data logger enabled the deformations of the front of the wall to be continuously monitored. One quarter of the wall was instrumented with LVDT's, their locations being shown in Figure 2.3 and 2.4. By assuming the walls behaved symmetrically, it was possible to determine the curvature along rows $R_1 - R_4$ or down columns $C_1 - C_5$ and, as with the wallettes, to use this information to determine the flexural rigidity and modulus of the material.

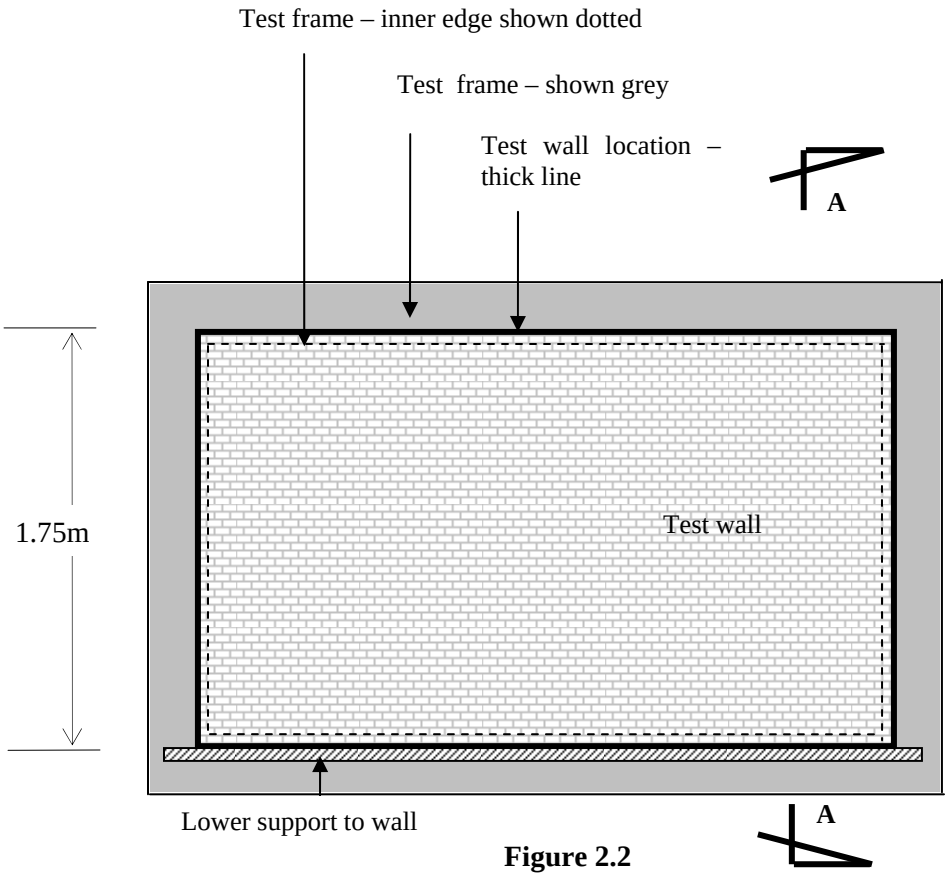

Figure 2.2
Rear elevation of wall not showing reaction frame

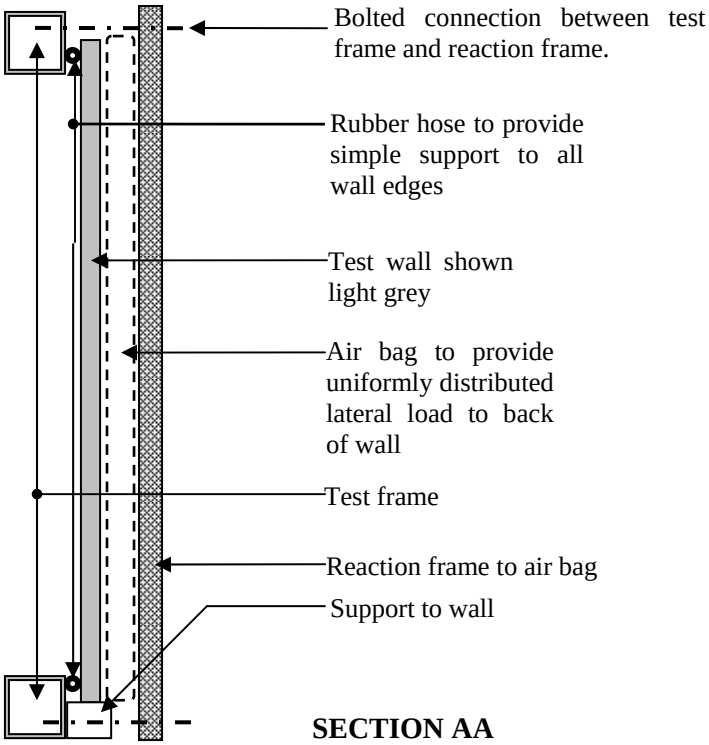

SECTION AA

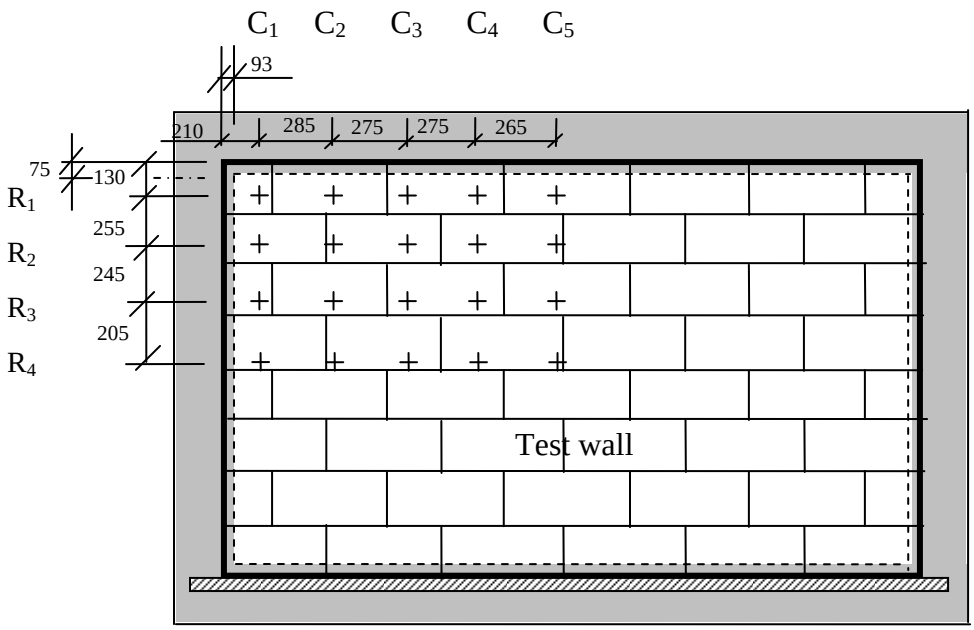

Figure 2.3 - GREY WALL
Location of LVDT's

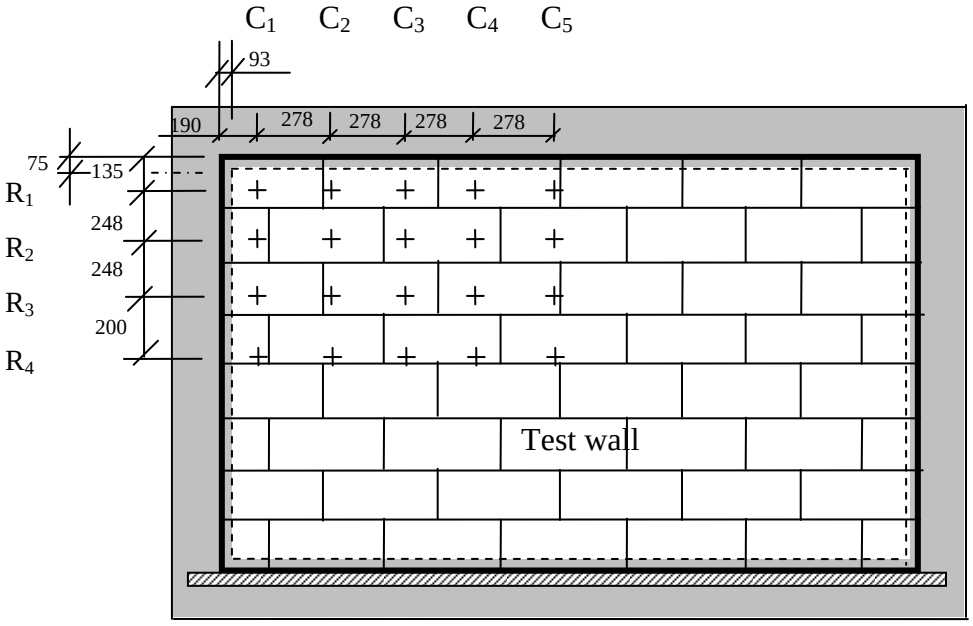

Figure 2.4 – YELLOW WALL
Location of LVDT's

3.0 RESULTS AND ANALYSIS

3.1 WALLETTES

For Grey wallettes tested in vertical bending (bending leading to failure in a plane parallel to the bed joints), the failure plane generally ran through the units. In a few cases, however, failure initiated in the interface between the unit and the mortar, but progressed through the units. It is thought that failure may have initiated in the joint probably at locations without full mortar coverage but soon moved into the block adjacent to the joints as the joint strength increased. It appears that due to high flexural bond strength, the bed joints did not experience any failure.

For Grey wallettes tested in horizontal bending (bending leading to failure in a plane perpendicular to the bed joints), all wallettes failed by developing cracks that ran almost vertically through a combination of units and head joints. Close observation revealed that although the failure plane ran very close to the perpend joints, there was actually very little de-bonding between the units and the mortar. As in vertical bending, failure was almost entirely through the units, indicating that the modulus of rupture of the units is less than the tensile flexural bond strength between the units and the mortar.

Yellow-block wallettes tested in vertical bending failed by a combination of de-bonding and unit failure. Failure initiated in the interface between the unit and the mortar, but progressed through the units. There was more de-bonding in the yellow-block wallettes than in the corresponding test involving Grey blocks.

For Yellow wallettes tested in horizontal bending, failure cracks ran almost vertically through units and head joints. Close observation, however, revealed that, unlike with the grey blocks, there was interface de-bonding between units and mortar in alternate courses, indicating that the bond in the yellow blocks was not as strong as that in the grey units, which means the modulus of rupture of the units may not be less than the tensile flexural bond strength between the units and the mortar. It appears that the wallette initially behaves as a plate, but de-bonding up the perpends at relatively low loads results in all the load being carried by the flexural capacity of the remaining units bridging the perpend joints. Clearly, some load is also carried by the torsional resistance of the bed joints even though none of the bed joints failed when wallettes were tested in the horizontal bending position.

Load vs. displacement relationships for three of four series of wallette tests described above are shown in Figure 3.1 – 3.3. Note that six wallettes formed each series of tests. No Load-Deflection results were recorded for the yellow B-wallettes. It is observed that all of the graphs are nearly linear from the initial application of the load up to about one third (33%) of the ultimate load. For the range between one third and two thirds of the ultimate load, the graphs have an upward concave curvature. In the final third of the load range, the graphs again become almost linear, with steeper slopes. When the failure strengths were reached, the wallettes failed instantaneously with an immediate and complete loss of strength.

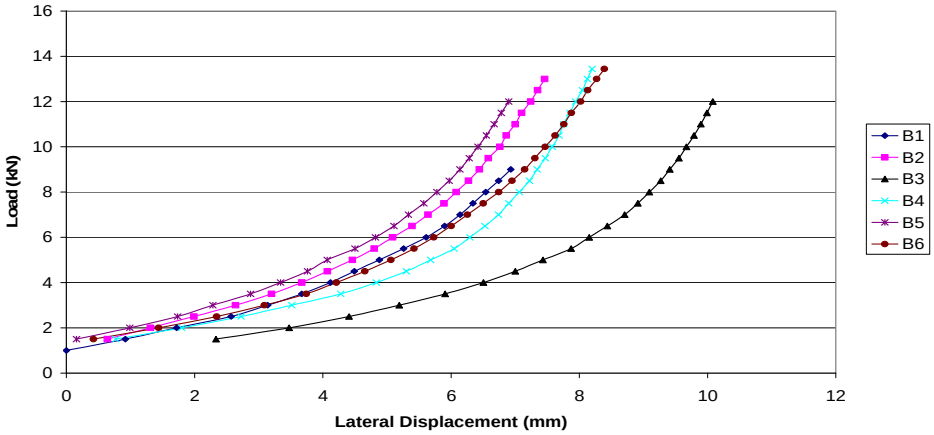

Figure 3.1: Load versus Displacement relationships for Grey B-wallettes (tested in vertical bending).

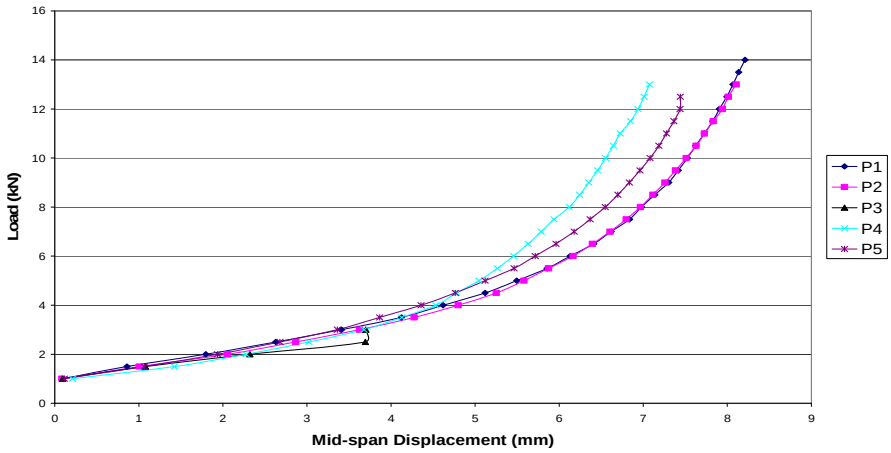

Figure 3.2: Load versus Displacement relationships for Grey P-wallettes (tested in horizontal bending).

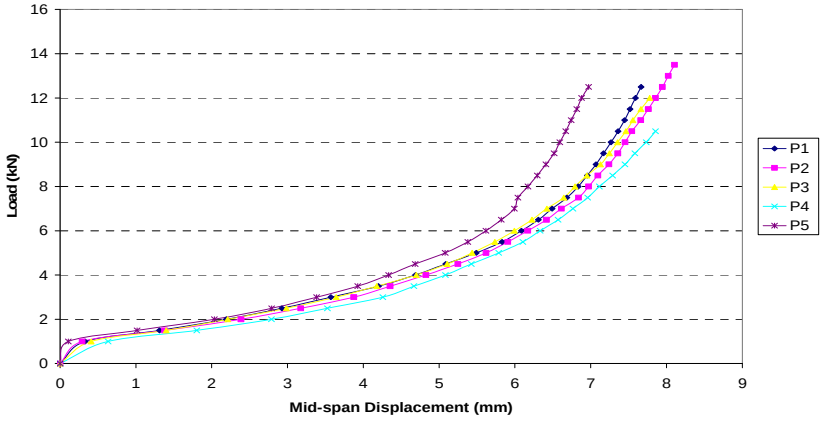

Figure 3.3: Load versus Displacement relationships for Yellow P-wallettes (tested in horizontal bending).

Figure 3.4 and Figure 3.5 show 'load versus displacement' relationships for P-wallette number 6, Grey and Yellow, respectively. For these wallettes, load was applied in three cycles: from 0 to 6 kN and then unloaded to 1 kN; then re-loaded up to 6 kN and unloaded again to 1 kN; and finally reloaded to failure. The graphs show that for the first cycle, the load-displacement relationship is almost linear up to about 4 kN for the Grey wallette, and 3.5 kN for the Yellow, thereafter becoming non-linear. For the second cycle, the graph is almost linear only up to about 3.0 kN for the Grey and 2.5 kN for the Yellow, and becomes non-linear for the rest of the loading history. There are, however, two linear sections for the final loading cycle; 0 – 2.5 kN, and 8 – 12 kN for the Grey wallette, and 0 – 2.5 kN and 8 – 11 kN for the Yellow. In between these linear regions, the graphs are non-linear, with an upward concave curvature. Failure of the wallettes, which resulted in complete loss of strength, was reached at 20 kN for Grey and 11.5 for Yellow wallette. Instrumentation was removed from the Grey wallette when a load of 12 kN was reached, for safety reasons.

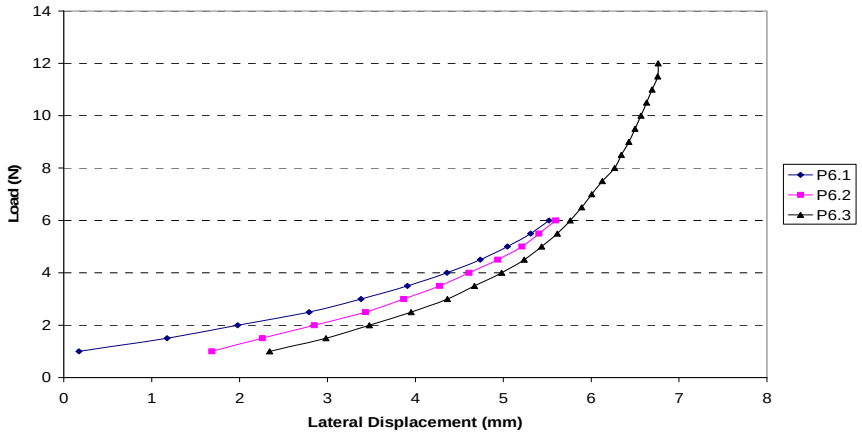

Figure 3.4: Load versus Displacement relationship for Grey P-wallette no.6

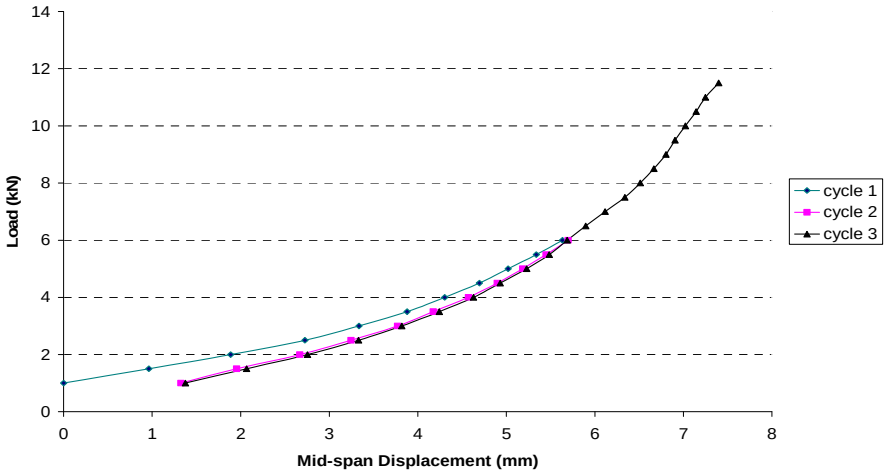

Figure 3.5: Load vs. Displacement graphs for Yellow P-wallette no.6

The Load/Deformation graphs for the block wallettes tested in this project clearly differ from typical graphs obtained for wallettes built from conventional mortars. Typical load-deflection

response of conventionally constructed block wallettes is shown in Figure 3.6, alongside a typical graph obtained in this study. According to Karihaloo [4], the initial linear elastic relationship in the graph of conventional masonry is due to the fact that under low tensile stresses, cracks have not yet formed in the material, or if they have formed, their influence on the mechanical response of the material is not noticeable. With an increase in applied tensile stress, micro-cracks form at the mortar/block interface leading to non-linearity and stiffness reduction in region AB in Figure 3.6(a). In contrast to this, thin-jointed block wallettes tested in this work exhibited linear (OA) – non-linear (AB) – linear (BC) behaviour, see Figure 3.6(b). Of paramount importance is the stiffness gain in the non-linear region. The stiffness gradually increases until it reaches a certain value (point B in Figure 3.6(b)), and maintains this value until the failure stress is reached. It may be argued, therefore, that during initial stages of application of the load (region OA, Figure 3.6(b)) there is very little micro-cracking, if any, in the material. It is postulated that the non-linear region of the graph (region AB, Figure 3.6(b)) is a result of some weaker parts of the bond progressively failing, while the stronger parts are just beginning to get involved in the response of the joint, hence the observed stiffness enhancement. It appears, therefore, that when forming mortar joints using thin joint technology, the strength of bonding over the face varies. With load, the weaker areas fail but, overall, the remaining bond is stronger and stiffer than the failed parts, resulting in the unusual behaviour. With the grey units, the remaining stronger areas of bond are even stronger than the units, resulting in the units rupturing before de-bonding can take place. For the yellow units, the bond strength appears to be less than the Unit Modulus of Rupture (UMOR) of the units since de-bonding is visibly evident. With both units the weaker parts of the joint do not contribute significantly to its strength.

Considering Figure 3.4 and 3.5, which show the relationship between load and deflection when loading and unloading a wallette 3 times, and eventually loading it to failure, some degree of elastic behaviour for the material is suggested, since on removal of the load there is some strain recovery. However, not all of the strain is regained, which also suggests some plastic strains. It could be that cracks start developing in the material at low stress values, but failure is initiated only when a certain crack width is reached. Therefore, the increase of non-linear behaviour in cycles 2 and 3 could be due to the material degrading, probably due to the formation of micro-cracks in the blocks and at the block/mortar interface, which can not be seen by the naked eye. Initially, there are no micro cracks but, with the addition of lateral pressure, they start forming, and with subsequent unloading the cracks do not fully close and therefore the strain cannot be fully recovered. During the second cycle, it takes less energy to deflect the wall equivalent distances as cracks exist from load cycle 1 and more cracks start forming at lower loads and hence there is a shorter linear section to the graph. In the final cycle, the cracks from load cycles 1 and 2 are sufficient to ensure there is even shorter linear portion at the start of cycle 3. The graph then becomes non-linear, but becomes linear again at higher stresses until failure occurs. This behaviour was discussed earlier.

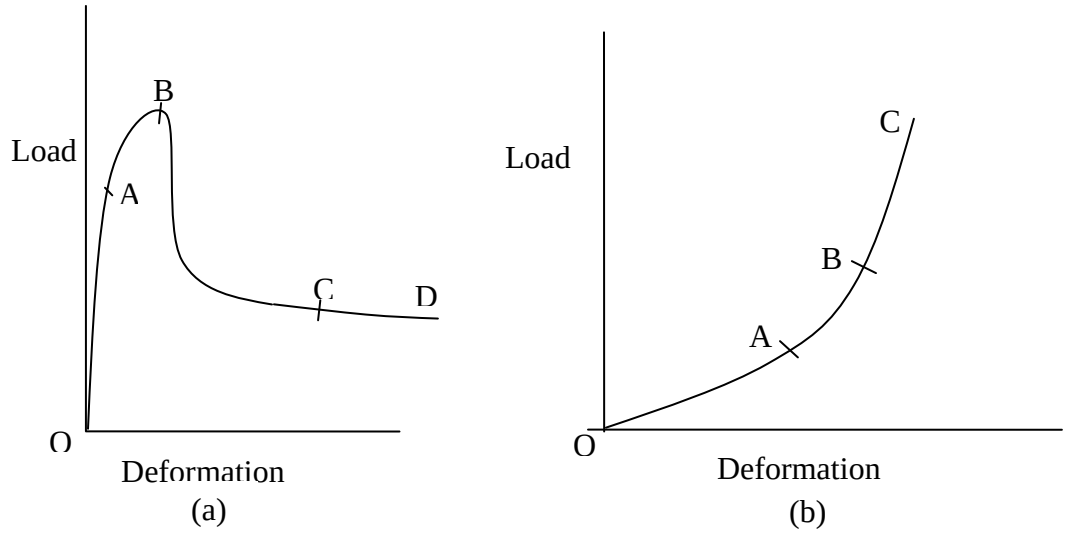

Figure 3.6: Typical Load-Deformation responses of laterally loaded masonry panels for tension in the direction parallel to the bed joints, built using: (a) conventional mortar, and (b) thin layer mortar.

3.2 WALL PANELS

3.2.1 GREY WALL

The initial crack in the grey wall occurred at a uniformly distributed load of 7.2kN/m^2 and a central deflection of 7.56 mm, and affected the left half of the wall. The crack occurred instantaneously and immediately the central deflection increased to 11.19 mm resulting in a pressure drop. The pressure was then increased and a second crack occurred at the same load of 7.2kN/m^2 and a deflection of 13.04 mm. This crack affected the right hand side of the panel, was again instantaneous and resulted in the deflection increasing to 16.37 mm with a corresponding pressure loss. At this point the LVDT's were removed and central deflection was estimated from this point forward. A third and fourth crack occurred at loads of 6.9 and 7.9kN/m^2 respectively, and with both cracks, the wall shifted outwards and there was a pressure loss to 4.2 kN/m^2. Thereafter, increasing deflections occurred under a reasonably constant pressure of 4.2kN/m^2.

Figure 3.7 shows the relationship between load and deflection at the centre of the wall, and the wall crack pattern is shown in Figure 3.8.

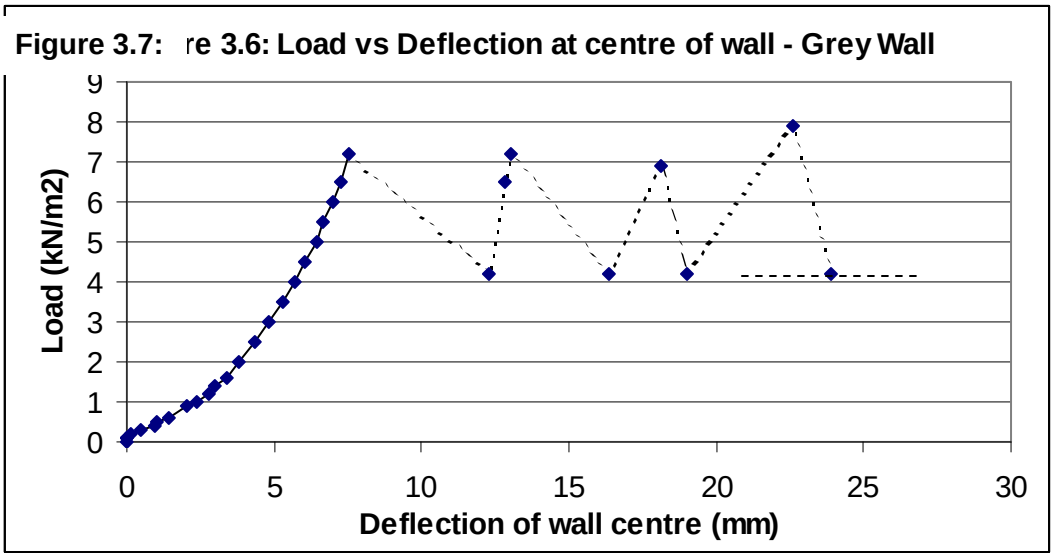

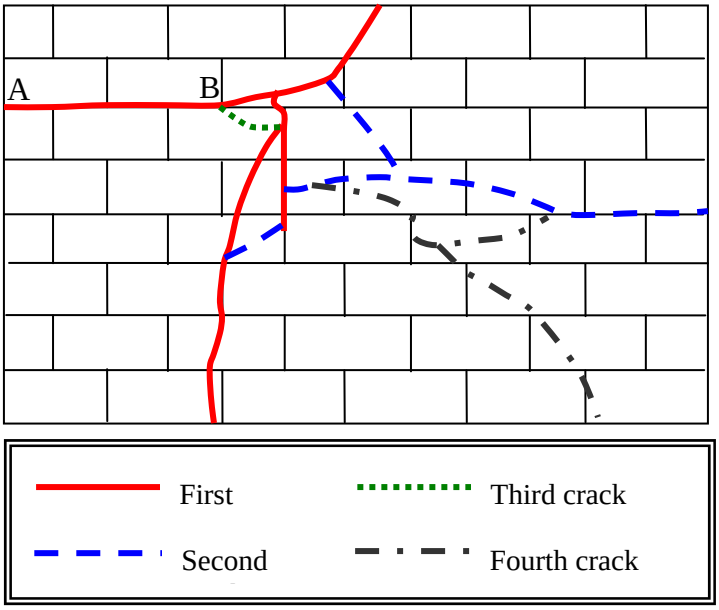

Figure 3.8: Crack pattern - Grey wall

The first set of cracks divided the wall into three sub-panels, as shown by the sketch in Figure 3.9(a). Each of Sub-panels 1 and 2 (Figure 3.9(a)) is supported along two edges and is relatively small compared to sub-panel 3. Therefore, the capacity of each of these sub-panels is likely to be higher than that of sub-panel 3. Sub-panel 3, on the other hand, is supported along 3 edges and free along the fourth (with only frictional shear stresses occurring along the crack line). Due to the differences of stiffness of the sub-panels, when further load was applied to the wall after the formation of the first crack, only sub-panel 3 failed, resulting in the formation of 'second crack' described in Figure 3.8. Figure 3.9(b) shows the typical crack patterns that have been observed when similar tests are done on conventional masonry.

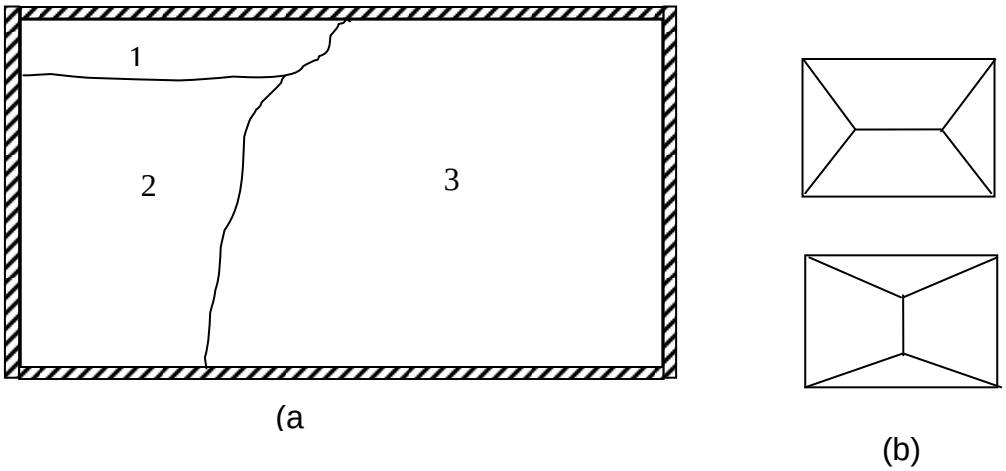

Figure 3.9: (a) Sketch showing three sub-panels of the grey wall after the first crack pattern occurred. (b) typical crack patterns in the case of conventional masonry.

Crack pattern 2 also divided sub-panel 3 into smaller sub-panels, 3a and 3b in Figure 3.10(a), each of which is supported along two adjacent edges. Sub-panel 3b, being the larger and therefore less stiff of the two, then failed by developing a crack that emanated very close to the intersection of the supported edges. This crack, which was referred to as 'forth crack' in Figure 3.8, is shown in the sketch of sub-panel 3b in Figure 3.11. Figure 3.11(b) shows the typical crack pattern that has been observed when similar tests are done on conventional masonry.

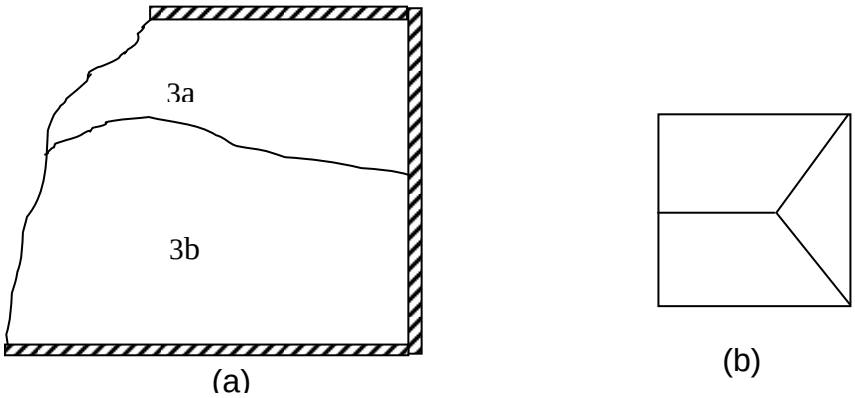

Figure 3.10: (a) A sketch of subsequent crack pattern of sub-panel 3 from figure 3.9. (b) typical crack pattern in the case of conventional masonry.

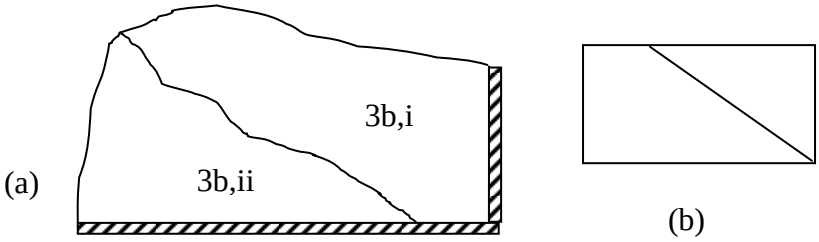

Figure 3.11: (a) Sub-division of sub-panel 3b into sub-panels 3b,i and 3b,ii. (b) typical crack pattern in the case of conventional masonry.

3.2.2 YELLOW WALL

Failure of the Yellow wall occurred in two stages. The first crack appeared instantaneously in the wall at a load of 6.0kN/m^2, and a central deflection of 7.74 mm. This crack pattern consisted of a horizontal crack at mid-height, running across the entire span, and two vertical cracks that initiated from the horizontal crack and terminated at the top and bottom edges of the panel. The second stage of cracking moved the wall outwards to a new deflection of 15.82 mm. At this point the cracks had widened and the pressure dropped to 2.9kN/m^2, but was subsequently increased to 4.0kN/m^2. The test was terminated with a central deflection of 21.05 mm and wider cracks, without any other crack pattern having formed.

The relationship between load and deflection at the centre of the wall is shown is Figure 3.12, and the wall crack pattern is shown in Figure 3.13.

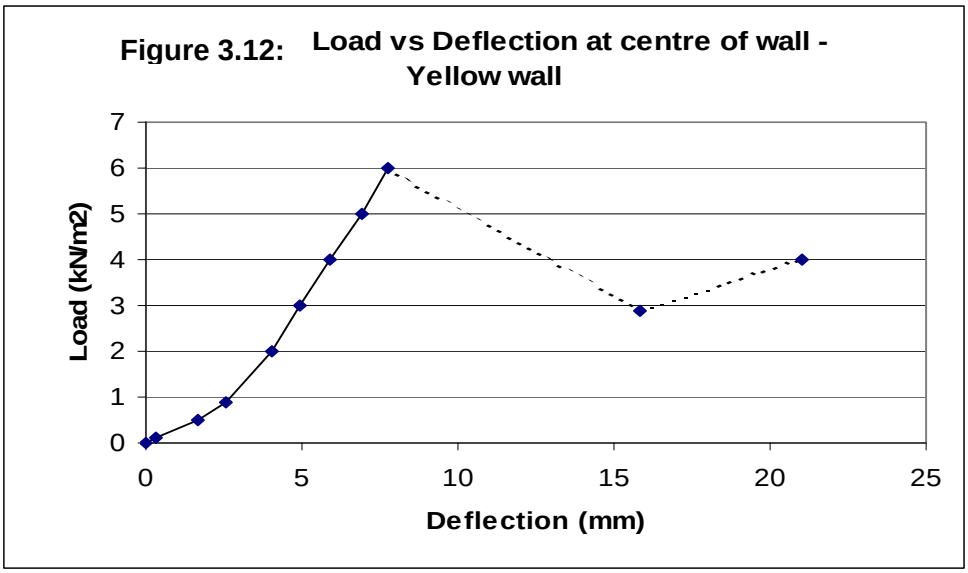

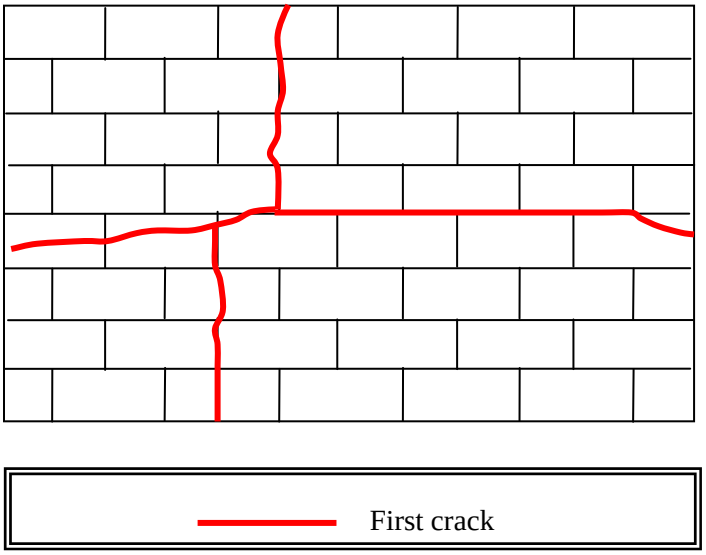

Figure 3.13: Crack pattern – yellow wall

It is very important to note that crack patterns of both Grey and Yellow walls resembled those of the corresponding wallettes. In the Grey wall cracks did not follow any pattern and generally ran through the units, proving that the mortar joints were stronger than the units. In the Yellow wall, however, the cracks initiated in the joints, but then spread into the units, revealing that the joints might be slightly weaker than the units. Another significant observation is that the Load versus Deflection graph of the wall centre, for both walls, is similar to the graphs obtained from the wallettes. This shows a consistency of results for the behaviour of this masonry type.

6.0 CONCLUSIONS

The following conclusions are drawn from the work that has been presented in this paper.

1. Load capacity of walls built using thin joint technology in conjunction with solid dense concrete blocks is considerably higher than when walls are built using conventional mortar.
2. Thin layer blockwork reveals more elastic properties than conventional masonry and, therefore, a design procedure based on elastic theory is likely to provide a solution.
3. Flexural test data for thin jointed blockwork has less variability than conventional masonry data. This will lead to a more reliable analytical model, and a design procedure that incorporates smaller values of safety factors.

ACKNOWLEDGEMENTS

This project was supported by Hanson Building Products, who supplied and built all the specimens and provided valuable guidance for which thanks are offered. In particular, the support of Paul Ragatski of Hanson Building Products is acknowledged. Thanks are also offered to Colin Bradsell, Peter Wells and Ron Adey of Kingston University for their technical assistance.

REFERENCES

1. BS 5628: Part 1, Code of Practice for Use of masonry, British Standards Institute, 1992.
2. BS DD ENV 1996, Eurocode 6: Design of Masonry Structures – Part 2
3. Fried, A.N., Roberts, J.J., Limbachiya, M.C., and Ahmed, A., “Thin Joint Masonry in the UK”, Masonry International, Vol. 18, No.2, August 2005, pp.85 -88.
4. Karihaloo, B.L., Fracture Mechanics and Structural Concrete, Longman Scientific & Technical, Essex, England, 1995
5. Hughes, T.G., Baker, M.G., and Harvey, R.J., “Tensile Strengths of Masonry Components”, Masonry International, The British Masonry Society, Volume 13, No.2, 2000, pp.39-43.